GHGT-10

Depressurization of carbon dioxide in pipelines – models and methods

Halvor Lund, Tore Flåtten, Svend Tollak Munkejord*

SINTEF Energy Research, Sem Sælands veg 11, NO-7465 Trondheim, Norway

Abstract

A model for two-phase carbon dioxide transport with phase transfer in pipelines is presented. The stiffened-gas equation of state is used for calculating thermodynamical properties. The convergence and accuracy of two numerical methods – a centred multi-stage (MUSTA) scheme and an upwind Roe scheme – are compared. Results for the depressurization of a pipe, causing phase change and cooling, are presented, showing the importance of an accurate numerical method. The effect of a discontinuous sound velocity on the depressurization is discussed.

1. Introduction

Carbon dioxide capture and storage (CCS) will potentially be an important contributor to reducing CO_2 emissions from stationary sources. According to the BLUE map of the International Energy Agency (IEA) [1], CCS will account for 19% of CO_2 emission reductions in 2050, equivalent to 9 gigatonnes per year. An important part of a CCS system is the transport between the point of capture and point of storage, which potentially can be far apart. Possible transport alternatives are ships and pipelines, and this work concerns the latter.

The carbon dioxide pipe transport will take place at high pressures, where the CO_2 is in a supercritical (liquid-like) state. Due to failure or planned maintenance, the pipe may be depressurized. The decreasing pressure will cause a phase change in the CO_2, leading to a strong cooling of the pipe. If the temperature becomes low enough, the pipe steel turns brittle, which may cause a rupture and severe damage. Therefore, it is important to be able to estimate the temperature drop during such a depressurization. When simulating the behaviour of a CO_2 pipe, we need fluid-mechanical and thermodynamic models to describe the flow, and numerical methods to properly solve these models. Therefore, we may experience errors with two seperate causes:

1. Modelling errors, i.e. failure of the fluid-dynamical or thermodynamic models to accurately represent the actual physics;

---

* Corresponding author: Tel: +47 73 59 38 97; fax: +47 73 59 28 89.
E-mail addresses: svend.t.munkejord@sintef.no, stm@pvv.org

2. Numerical errors, i.e. failure of the numerical method to solve the models with a satisfactory degree of accuracy.

In this work, we will show that even with accurate mathematical models, numerical errors can greatly influence the simulation results for a CO_2 pipe.

The flow models of interest are typically formulated as systems of hyperbolic partial differential equations. It is well-known that artifical numerical diffusion, needed to stabilize the solution of such equations, may lead to severe loss of accuracy. To demonstrate how the choice of numerical method affects the solution, we compare an upwind high-resolution scheme with a centred first-order scheme, namely the MUSTA (multi-stage) scheme previously investigated for the current model [2]. The model is a drift-flux two-phase flow model, in which each chemical component is explicitly tracked.

Our upwind scheme is based on the approximate Riemann solver of Roe [3], and high resolution is obtained by the wave-limiter approach of LeVeque [4], Chap. 15. The present Roe scheme has previously been employed in a case where phase transfer (evaporation) was not accounted for [5]. During the depressurization of a pipe, phase change will clearly take place. In this article, we therefore show that our Roe scheme is applicable to the case where more complex thermodynamical relations are employed for calculating phase equilibria in two-phase mixtures involving CO_2.

The paper is organized as follows: In Section 2, we present the model we use to describe the pipeline flow of CO_2 with phase transfer, composed of a fluid-dynamical and a thermodynamical model. Section 3 describes the two numerical methods used to implement the model and perform simulations, while Section 4 shows simulation results for a pipe depressurization case, demonstrating convergence and accuracy of the two methods. Finally, Section 5 summarizes and concludes the results of our work.

2. Models

When we choose a model to represent the physics mathematically, simplifications are most often necessary. Such simplifications may ease the numerical implementation of the model or ease the analytical understanding of it. The choice of which simplifications to make is a compromise between which physical properties we want the model to capture, and how simple we wish the model to be.

Our model describes a flow of a single component, e.g. CO_2, which can appear in two phases, liquid and vapour. We choose to make certain equilibrium assumptions:

- mechanical/pressure: $p_g = p_l = p$
- thermal/temperature: $T_g = T_l = T$
- chemical potential: $\mu_g = \mu_l = \mu$

Here, the subscript g denotes gas and the subscript l denotes liquid. The last equilibrium condition imposes equal chemical potential (i.e. Gibbs free energy) in the two phases. This implies an instant phase transfer to reach equilibrium, similar to flash evaporation. A model with these three equilibrium assumptions is known as a homogeneous equilibrium model [6].

The complete model can be considered to be composed of two parts: fluid dynamics and thermodynamics.

2.1. Fluid dynamics

The fluid-dynamical model should capture the most important aspects of flow of CO_2 in a pipeline. Since we are most interested in changes along the length of the pipe, we use a one-dimensional model. In addition, we assume that the velocity is equal in the two phases, i.e. a no-slip condition. The three equilibrium assumptions presented earlier make it possible to describe the two-phase flow using the Euler equations for a single fluid:

$$\frac{\partial \rho}{\partial t} + \frac{\partial \rho v}{\partial x} = 0, \tag{1}$$

$$\frac{\partial \rho v}{\partial t} + \frac{\partial (\rho v^2 + p)}{\partial x} = 0, \tag{2}$$

$$\frac{\partial E}{\partial t} + \frac{\partial [v(E+p)]}{\partial x} = 0, \tag{3}$$

where the total energy is written as $E = \rho(e + \frac{1}{2} v^2)$. These equations describe the conservation of mass, momentum and energy, respectively. The component is composed of two phases, so that the mixture density can be written as

$$\rho = \alpha_g \rho_g + \alpha_\ell \rho_\ell, \tag{4}$$

and the mixture internal energy as

$$e = \frac{\alpha_g \rho_g e_g + \alpha_\ell \rho_\ell e_\ell}{\rho}. \tag{5}$$

α_k is the volume fraction, e_k the internal energy, and ρ_k the density, of phase k. The equilibrium assumptions, together with the thermodynamical model, are sufficient to calculate volume fractions and pressure from the conserved variables.

2.2. Thermodynamics

To close the fluid-dynamical model, we need a relation for the pressure, p, as a function of mixture internal energy, e, and mixture density, ρ, subject to the equilibrium restrictions presented earlier.

We use the stiffened-gas equation of state (EOS), advocated by e.g. Menikoff [7, 8], as our thermodynamical model. The stiffened-gas EOS can be seen as a linearization of a more general EOS. It has the advantage of being simpler than most other EOSes, while still being relatively accurate in the vicinity of a chosen reference point.

The pressure, internal energy and chemical potential (for a single phase) are given by

$$p(\rho, T) = \rho(\gamma - 1)c_v T - p_\infty, \tag{6}$$

$$e(\rho, T) = c_v T + \frac{p_\infty}{\rho} + e_*, \tag{7}$$

$$\mu(\rho, T) = \gamma c_v T + e_* - c_v T \ln\left(\frac{T}{T_0}\left(\frac{\rho_0}{\rho}\right)^{\gamma-1}\right) - s_0 T, \tag{8}$$

where γ, c_v, p_∞, e_*, T_0, ρ_0 and s_0 are parameters specific for each phase. These parameters can be fitted using experimental data for a given fluid. The parameters used in this paper are listed in Table 1. The equations (6)-(8) have to be solved for pressure as a function of mixture internal energy and density, which in turn is used in the fluid-dynamical model. From the third term of the chemical potential (8), we realize that solving for T involves solving a transcendental equation, which means that an analytical solution is out of reach. Therefore, the pressure was solved numerically using a Newton method.

2.3. Sound velocity

The sound velocity is an important parameter in a depressurization case, because it determines how fast the pressure drop will propagate through the pipe. This velocity is dependent on the choice of both the thermodynamical and the fluid-dynamical model.

Saurel et al. [9] showed that the sound velocity c_{eq} in the homogeneous equilibrium model is given by

$$c_{eq}^2 = \frac{1}{\rho}\left(\frac{\alpha_g}{\rho_g c_g^2} + \frac{\alpha_\ell}{\rho_\ell c_\ell^2} + T\left[\frac{\alpha_g \rho_g}{c_{p,g}}\left(\frac{ds_g}{dp}\right)^2 + \frac{\alpha_\ell \rho_\ell}{c_{p,\ell}}\left(\frac{ds_\ell}{dp}\right)^2\right]\right)^{-1}, \tag{9}$$

where c_g and c_l are the sound velocities of pure gas and pure liquid, respectively. s_k is the entropy and $c_{p,k}$ the specific heat capacity at constant pressure, of phase k. The entropy derivatives are evaluated at the boiling curve.

An important note to make is that the sound velocity is discontinuous at the transition between a pure phase (either gas or liquid) and a two-phase mixture. That is, $c_{eq}(\alpha_l = 1) \neq c_l$ and $c_{eq}(\alpha_g = 1) \neq c_g$. This effect has not been observed experimentally, see e.g. Coste et al. [10] or Kieffer [11], hence it is probably not an actual physical effect. Figure 1 shows the sound velocities of three different models, with increasing degree of equilibrium in pressure, temperature and chemical equilibrium. In this figure we clearly see that the model with full equilibrium has a far lower sound velocity than models without chemical equilibrium. However, the advantage with the homogeneous equilibrium model is that no explicit modelling of phase transfer is required.
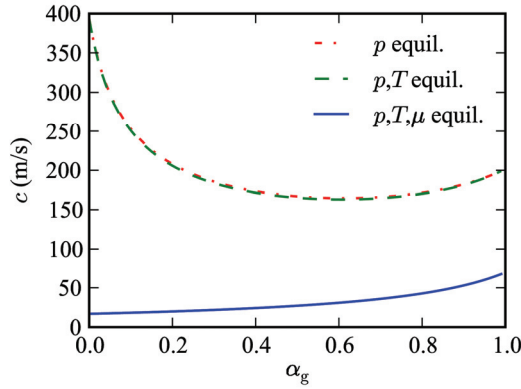
Figure 1: Sound velocity as a function of gas volume fraction for models with different equilibrium assumptions.

Table 1: CO_2 parameters for the stiffened-gas equation of state.

	Gas	Liquid
γ	1.044	1.157
c_v (J/kg K)	3075	2955
p_∞ (Pa)	$1.140 \cdot 10^6$	$1.046 \cdot 10^8$
e_* (J/kg)	$-5.077 \cdot 10^5$	$-7.451 \cdot 10^5$
T_0 (K)	288	288
ρ_0 (kg/m^3)	159.9	822.5
s_0 (J/kg K)	1750	1134

3. Numerical method

To solve the presented model numerically, we need a proper numerical method. First, we write the equation system (1)-(3) more compactly as

$$q_t + f(q)_x = 0, \tag{10}$$

where q is the vector of conserved variables, i.e.

$$q = (\rho, \rho v, E)^T, \tag{11}$$

and $f(q)$ is the flux function,

$$f(q) = (\rho v, \rho v^2 + p, v(E + p))^T. \tag{12}$$

An equation system in the form (10) can be solved with a finite-volume scheme, in which one divides the domain into control volumes. By integrating the equation over x, we get

$$\frac{dQ_i}{dt} = -\frac{1}{\Delta x}(F_{i+1/2} - F_{i-1/2}), \tag{13}$$

where Q_i is the integral of q over volume i. $F_{i+1/2}$ is the flux between cell i and $i+1$. Using the Forward Euler method for integrating in time yields where the superscript m indicates a quantity evaluated at time t_m.

$$Q_i^{m+1} - Q_i^m = -\frac{\Delta t}{\Delta x}(F_{i+1/2}^m - F_{i-1/2}^m), \tag{14}$$

The challenge in solving (14) lies in calculating the flux function $F_{i+1/2}$ at the cell interface, knowing only Q_i and Q_{i+1}, the integral of q in the neighbouring cells. Two classes of methods for solving such problems are centred schemes and upwind schemes. In the following, we present one scheme of each type: a centred MUSTA scheme and an upwind Roe scheme.

3.1. Roe scheme

The Roe method [3] is based on transforming the differential equations (10) to a quasi-linear system in the form

$$q_t + \hat{A}_{i+1/2}q_x = 0, \tag{15}$$

which applies to the cell interface between cell i and $i+1$. The matrix $\hat{A}_{i+1/2}$ is a function of q in these two cells, denoted q_L (left) and q_R (right). The matrix is then used to find the flux $F_{i+1/2}$.

A challenge in developing a Roe scheme lies in constructing the matrix $\hat{A}_{i+1/2}$, which has to have the following properties:

1. $\hat{A}_{i+1/2}(q_L, q_R)(q_R - q_L) = f(q_R) - f(q_L)$
2. $\hat{A}_{i+1/2}(q_L, q_R)$ is diagonalizable with real eigenvalues
3. $\hat{A}_{i+1/2}(q_L, q_R) \to \partial f / \partial q_L$ as $q_R \to q_L$

These criteria ensure that the scheme is conservative, hyperbolic, and consistent with the original equation system (10), respectively. The first criterion is typically the hardest to satisfy. Morin et al. [5] constructed a Roe scheme for a model with an arbitrary number of components with common pressure, velocity and temperature. This scheme can handle any thermodynamic model, thus it is suitable for our case.

The eigenstructure of the Roe matrix is used to resolve and propagate the individual waves at each cell interface. This involves diagonalizing the matrix, which in our case is done numerically. To achieve a higher-order method, we employ the wave-limiter approach of LeVeque [4], Chap. 15. This yields a second-order method where the solution is smooth. We choose to use the Superbee limiter [12].

3.2. MUSTA scheme

The multi-stage centred (MUSTA) scheme was proposed by Toro and coworkers [13, 14]. Centred schemes are simpler than upwind schemes, since centred schemes do not have to resolve the eigenstructure of the equation system. In other words, the flux function $F_{i+1/2}$ is calculated without considering the direction in which the waves are travelling. The MUSTA scheme uses the FORCE flux function [15], which is an average of the Lax-Friedrichs and Richtmyer fluxes.

The MUSTA scheme is based on solving the problem (14) at each cell interface on a local grid, and then use the local solution in the global grid. When the number of grid cells and time steps in the local grid is increased, the accuracy approaches that of upwind schemes, while the scheme retains the simplicity of centred schemes. The MUSTA scheme we use is similar to the one used by Munkejord et al. [2], and all simulations will be run using two local time steps and two local grid cells.

4. Depressurization results

We will now show results from simulation of depressurization of a pipe of length $L = 100$ m with pure CO_2. The initial conditions inside the pipe are a pressure at $p_0 = 60$ bar, temperature at $T_0 = 288$ K ≈ 15 °C, and zero velocity. At these conditions, CO_2 is in the liquid phase. The parameters for the stiffened-gas EOS are listed in Table 1.

At time $t = 0$, the right end ($x = 100$ m) of the pipe is opened and exposed to an external pressure of $p_e = 30$ bar. This causes a depressurization wave to propagate through the pipe, causing the fluid to flow towards the right end. The decreasing pressure will cause some of the liquid to evaporate, and hence a temperature drop. All simulation results are shown at time $t = 0.2$ s. The Courant-Friedrichs-Lewy (CFL) number used was 0.9.

4.1. Convergence

First, we show how the solution converges as the grid is refined. The number of grid cells is varied from 50 to 6400 cells. For a proper numerical method, increasing the number of grid cells, i.e. decreasing the size of each cell, should not cause any oscillations. We choose to show the temperature and volume fraction for 85 m $< x <$ 100 m, as the results in this region illustrate the convergence well.

Figure 2 shows convergence test results for the Roe method with Superbee limiter, abbreviated Roe SB. We see that the solution converges nicely without any oscillations or other artifacts. Results for the same test for the MUSTA method are shown in Figure 3. Also this method converges nicely, although with slightly less sharp corners. This is to be expected, since centred methods are more diffusive than upwind methods. These results confirm that both methods will converge to the same solution.

The convergence to the same solution is illustrated even more clearly in Figure 4, where the solutions for MUSTA and Roe SB with a very fine grid are shown. Even with 25600 cells, it is still possible to see how MUSTA smears the sharp corners of the depressurization wave.

Figure 5 shows results for the two methods compared, in addition to the Roe method without any wave-limiting. We see that MUSTA and Roe without limiting have comparable results. The higher-order Roe SB is far closer to the converged solution. We can also see, especially from Fig. 3(a), that the MUSTA method underestimates the temperature drop to a much larger degree than Roe SB. This illustrates the importance of a higher-order method for obtaining sufficient accuracy in a depressurization calculation.
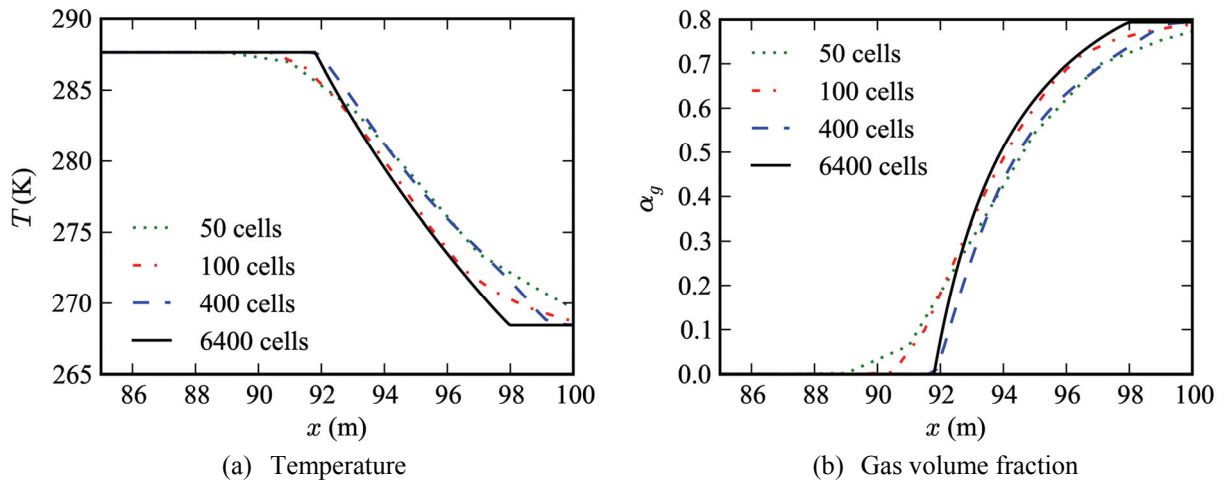
(a) Temperature

(b) Gas volume fraction

Figure 2: Convergence test for the Roe method with Superbee limiter (Roe SB). Note that only the right-most part of the domain is shown
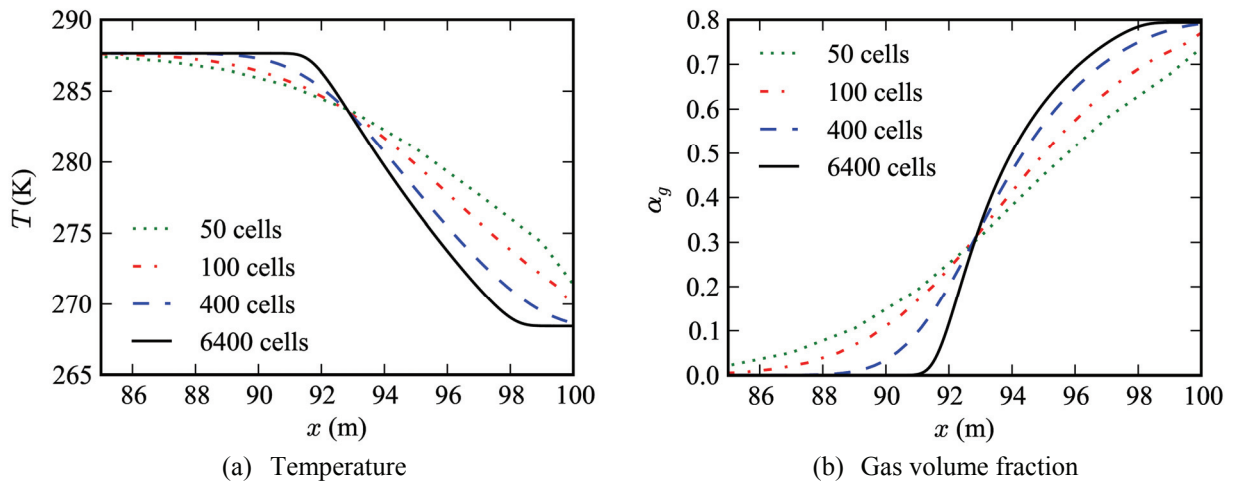

(a) Temperature

(b) Gas volume fraction

Figure 3: Convergence test for the MUSTA method. Note that only the right-most part of the domain is shown.

(a) Temperature

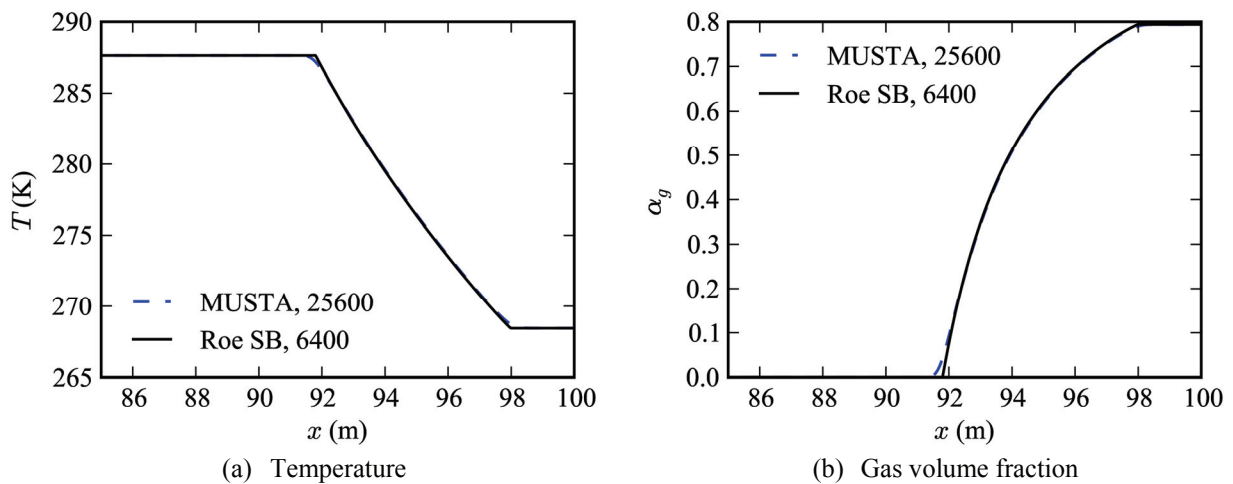(b) Gas volume fraction

Figure 4: Solution with very fine grid for MUSTA and Roe SB.
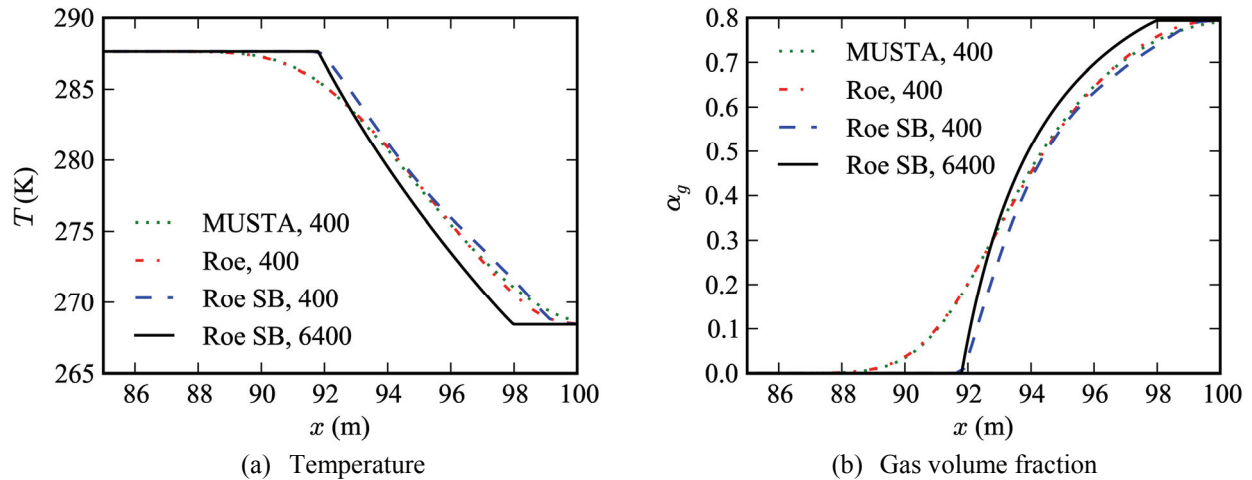
(a) Temperature

(b) Gas volume fraction

Figure 5: Comparison of convergence for the different methods. Note that only the right-most part of the domain is shown.
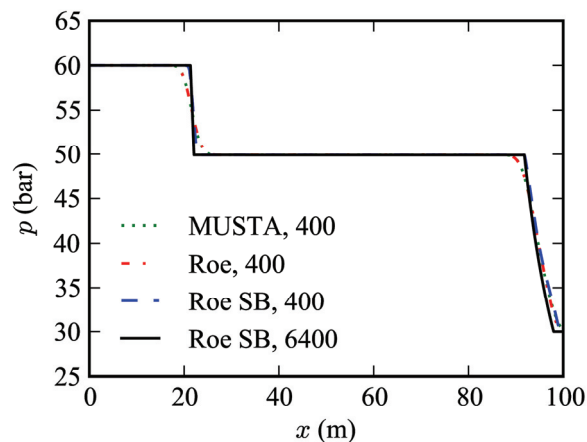

Figure 6: Pressure during a depressurization.

4.2. Effects of discontinuous sound velocity

As seen in Figure 6, the depressurization (or rarefaction) wave caused by the low pressure at the end of the pipe is split into two parts. The first (left) part is a pressure drop from the initial pressure to the saturation pressure at $p \approx 50$ bar. The second (right) part is where the evaporation starts to occur. These two waves are split because of the discontinuous sound velocity, which causes the pressure wave in the two-phase mixture to propagate much slower as soon as evaporation begins, as noted in Section 2.3 and Fig. 1. The speed of sound is $c_l \approx 450$ m/s in pure liquid, while the two-phase mixture has a speed as low as $c_{mix} \approx 25$ m/s. This also means that the temperature drop due to phase change will take longer to reach into the pipe, than in a model without equilibrium in chemical potential.

For a depressurization case, the velocity of pressure waves (i.e. sound velocity) is an important parameter, so the choice of model is an important one. Instead of the model presented in this paper, one could use a model with equilibrium in only temperature and pressure, with mass transfer as a source term in the mass equation. This model would not have a discontinuity in the sound velocity. However, a difficulty with mass transfer as a source term is the need to explicitly model it.

5. Conclusion

We have presented a model for two-phase flow of CO_2 with equilibrium in both pressure, temperature and chemical potential (also known as the homogeneous equilibrium model). Simulation results for a depressurization of a pipe was presented, demonstrating the accuracy and convergence of a (centred) MUSTA scheme and a (upwind) Roe scheme. It was seen that the MUSTA scheme has difficulty resolving the sharp edges of the depressurization wave due to its diffusivity. We have shown how a higher-order method like the Roe method with wave-limiting significantly improves the resolution of a depressurization wave.

Further work may model the phase transfer between the two phases using a mass-transfer term, yielding a sound velocity closer to experimental results. Such a model may be suitable for depressurization calculations. The Roe scheme used in this work and the work of Morin et al. [5] may also be used for such a model.

Acknowledgement

References

[1] IEA/OECD. Energy technology perspectives 2008, 2008.

[2] Svend Tollak Munkejord, Jana P. Jakobsen, Anders Austegard, and Mona J. Mølnvik. Thermo- and fluid-dynamical modelling of two-phase multi-component carbon dioxide mixtures. *International Journal of Greenhouse Gas Control*, 4:589–596, 2010.

[3] P. L. Roe. Approximate Riemann solvers, parameter vectors, and difference schemes. *Journal of Computational Physics*, 43:357–372, 1981.

[4] Randall J. LeVeque. *Finite Volume Methods for Hyperbolic Problems*. Cambridge University Press, 2002.

[5] Alexandre Morin, Peder Kristian Aursand, Tore Flåtten, and Svend Tollak Munkejord. Numerical resolution of CO2 transport dynamics. In *SIAM Conference on Mathematics for Industry: Challenges and Frontiers (MI09)*, San Francisco, CA, USA, October 9-10 2009.

[6] S. Clerc. Numerical simulation of the homogeneous equilibrium model for two-phase flows. *Journal of Computational Physics*, 161:354–375, 2000.

[7] R. Menikoff. Empirical equations of state for solids. *Shock Wave Science and Technology Reference Library*, 2:143–188, 2007.

[8] R. Menikoff and B. J. Plohr. The Riemann problem for fluid flow of real materials. *Rev. Mod. Phys.*, 61:75–130, 1989.

[9] Richard Saurel, Fabien Petitpas, and Rémi Abgrall. Modelling phase transition in metastable liquids: application to cavitating and flashing flows. *Journal of Fluid Mechanics*, 607:313–350, 2008.

[10] C. Coste, C. Laroche, and S. Fauve. Sound propagation in a liquid with vapor bubbles. *Europhysics Letters*, 11:343–347, 1990.

[11] Susan Werner Kieffer. Sound speed in liquid-gas mixtures: Water-air and water-steam. *Journal of Geophysical research*, 82(20):2895–2904, July 1977.

[12] P. L. Roe. Some contributions to the modeling of discontinuous flows. *Lect. Appl. Math.*, 22:163–193, 1985.

[13] V. A. Titarev and E. F. Toro. Musta schemes for multi-dimensional hyperbolic systems: analysis and improvements. *International journal for numerical methods in fluids*, 49:117–147, 2005.

[14] E. F. Toro. Multi-stage predictor-corrector fluxes for hyperbolic equations. In *Isaac Newton Institute for Mathematical Sciences Preprint Series*. University of Cambridge, UK, June 2003.

[15] E. F. Toro. On Glimm-related schemes for conservation laws, Technical Report MMU-9602. Technical report, Department of Mathematics and Physics, Manchester Metropolitan University, UK, 1996.